THE ASTROPHYSICAL JOURNAL, 364:540–548, 1990 December 1

STUDIES OF THE LOCAL INTERSTELLAR MEDIUM. VIII. MORPHOLOGY AND KINEMATICS OF THE DIFFUSE INTERSTELLAR CLOUDS TOWARD ORION

P. C. FRISCH,[1] K. SEMBACH, AND D. G. YORK[1,2]
Department of Astronomy and Astrophysics, University of Chicago
Received 1990 March 1; accepted 1990 May 30

ABSTRACT

Interstellar clouds in the direction of the Orion association show only positive velocities for target stars within 190 pc of the Sun, and both positive and negative velocities for more distant target stars, confirming an earlier prediction by Cowie, Songaila, and York. The nearby positive velocity cloud, designated here as Orion-Lepus 70 (OL 70), is a "standard" diffuse interstellar cloud: it is subject to the ambient galactic radiation field, with properties consistent with $T \sim 10^2$ K and $n \sim 3$ cm^{-3}. Combined with a column density $\log N(\mathrm{H}) = 19.8$–$20.0$ cm^{-2}, these values imply a cloud thickness of ~ 7 pc. The kinematics of OL 70 are consistent with either an origin as part of the expanding Loop I superbubble shell, or as part of Lindblad's expanding ring, or a synthesis of the two models. The negative velocity interstellar components seen in stars at $d \geq 200$ pc are caused by interstellar matter accelerated by the expanding Ori-Eri superbubble. Relatively dense interstellar gas at positive LSR velocities is also found within the Orion association, so that it is difficult to pick out OL 70 components in the spectra of the distant stars.

Subject headings: clusters: associations — interstellar: matter

I. INTRODUCTION

The relative absence of dense clouds for the first 100 pc of the sight line in front of the Orion OB I association and the apparent association of observed clouds in that direction with either the Orion association or superbubble suggest that between the interstellar cloud surrounding the Solar System and interstellar gas associated with Orion this sightline is "empty." Isolated observations of interstellar absorption features in stars at $d \sim 100$ pc towards Orion and Taurus, however, reveal interstellar gas at the velocity of the local interstellar flow velocity (Crutcher 1982; Frisch and York 1986). In this paper, optical observations of interstellar Ca II and Na I towards stars in Orion, Lepus, and Eridanus provide information on the kinematics of this interstellar cloud, which is interesting because it is in front of the Orion superbubble.

The diffuse gas in the Orion region has been extensively studied in the optical, radio, and ultraviolet regions of the spectrum. The Orion OB I association is 400–500 pc distant, and is well-known as an active region of sequential star formation (estimated age $\leq 15 \times 10^6$ yr, e.g., Warren and Hesser 1978) and for the Orion molecular clouds (e.g., Maddalena *et al.* 1986). Here stellar winds, intense UV radiation, and supernova activity have generated segments of ionized and neutral shells in the interstellar clouds surrounding the association. Portions of these shells were first observed in the red with the discovery in the early 1890's of an intense Hα emission feature now known as "Barnard's Loop" (Pickering 1890; Barnard 1895). Barnard's Loop is recognized as part of a large superbubble feature and has been studied in UV absorption lines (Cowie *et al.* 1979), optical absorption lines (Hobbs 1969, 1974, 1976, 1978*a*), radio H I 21 cm emission and Zeeman splitting (Menon 1958; Heiles 1976, 1984; Troland and Heiles 1982), radio continuum (Reich 1978), Hα and S II (Reynolds and Ogden 1979, hereafter RO; Sivan 1974; Sivan *et al.* 1986; Reynolds 1988; Isobe 1973), far-UV emission and soft X-ray emission (O'dell *et al.* 1967; Paresce *et al.* 1983; Nousek *et al.* 1982), and the polarization of starlight by interstellar dust grains (Appenzeller 1974). Barnard's Loop coincides with the tangential sightline through the superbubble perimeter, with the Hα emission following the inner edge of a dense H I shell.

The volume of space in front of the Orion OB association shows relatively little interstellar gas and dust (Lucke 1978; Perry *et al.* 1983; Bohlin *et al.* 1983; Hobbs 1987*a*; Frisch and York (1983). As a result, the interstellar gas towards the Orion OB association has a significantly lower value for the average spatial density n_{tot} [$n_{\mathrm{tot}}(\mathrm{cm}^{-3}) = n(\mathrm{H\,I}) + 2n(\mathrm{H_2})$] than towards the other nearby associations such as Sco-Cen and Per. For example, from the data of Bohlin *et al.* (1983), we see that the seven stars within the interval $l = 199°$ to $207°$ and $b = -17°$ to $-31°$ have $\langle n_{\mathrm{tot}} \rangle_{\mathrm{Orion}} = 0.29$ cm^{-3}, while the 21 stars for all of the rest of the sky have average spatial densities of $\langle n_{\mathrm{tot}} \rangle_{\mathrm{other}} = 0.48$ cm^{-3}. Apparently, reduced depletions for many elements seen in this direction have been related to these low-average spatial densities (e.g., Jenkins 1987). However, the effects of low-average spatial densities have not been unambiguously separated from the effects of high spatial density clouds positioned by coincidence in a sightline with relatively low total column densities.

The thrust of this paper is to understand the distribution and kinematics of the interstellar medium in this direction so that individual properties of these clouds, such as depletions, temperature, and density, can be derived independently of average sightline properties. This objective is accomplished by mapping clouds in this region using optical Ca II and Na I lines and ultimately comparing the Na I data with H I column densities in order to determine the spatial density of the cloud.

II. DATA

The target stars are listed in Table 1, and are plotted as squares in Figure 1 against a sketch of Barnard's Loop. (Other

[1] Visiting Astronomer, Kitt Peak National Observatory and Cerro-Tololo Inter-American Observatory, which are operated by The Association of Universities for Research in Astronomy, Inc., under contract with the National Science Foundation.

[2] Also, Enrico Fermi Institute, University of Chicago.

TABLE 1

TARGET STARS

Star	Name	Orion Association Subgroup	l	b	Spectral Type	Distance[a] (pc)	RV (km s^{-1})	$v \sin i$ (km s^{-1})	V	$B-V$
HD 32249.....	ψ Eri		206.6	−27.7	B3 V	188	25V	74	4.81	−0.19
HD 32964.....	66 Eri		204.8	−25.4	B9 V + A1 V	112	31SB20	41	5.12	−0.06
HD 33111.....	β Eri		205.3	−25.3	A3 III	26	−9	179	2.79	0.13
HD 33328.....	λ Eri		209.1	−26.7	B2 IVne	267	3V	336	4.27	−0.19
HD 33802.....	ι Lep		212.7	−27.3	B8 V	84	25V	193	4.45	−0.10
HD 33949.....	κ Lep		213.9	−27.6	B9 V	70	18V	124	4.36	−0.10
HD 34503.....	τ Ori		208.3	−24.0	B5 III	134	20SB	46	3.60	−0.11
HD 34816.....	λ Lep		214.8	−26.2	B0.5 IV	507	20	67	4.29	−0.26
HD 34863.....	ν Lep		214.0	−25.8	B7 IVnn	187	16	370	5.30	−0.12
HD 35039.....	22 Ori	Ia	202.6	−20.0	B2 IV-V	404	29SB1?	14	4.73	−0.17
HD 35149.....	23 Ori	Ia	199.2	−17.9	B1 V	404	18	295	5.00	−0.15
HD 35411.....	η Ori	Ia	204.9	−20.4	B1 V + B2e	404	20SB20	46	3.36	−0.17
HD 35468.....	γ Ori		196.9	−16.0	B2 III	124	18SB?	59	1.64	−0.22
HD 36486.....	δ Ori	Ib3	203.9	−17.7	B0 III + O9 V	406	16SB0	152	2.23	−0.22
HD 36727.....			212.6	−21.6	A9 V[b]	224–282		47:[c]	8.70	0.20
HD 37079.....			212.1	−20.8	B9.5 V[b]	240–292			8.00	0.10
HD 37128.....	ϵ Ori	Ib2	205.2	−17.2	B0 Iae	427	26SB	87	1.70	−0.19
HD 37358.....			212.0	−20.1	A4 V[b]	192–234		88[c]	8.00	0.10
HD 37492.....		Ic[d]	212.3	−20.0	B9 IV	439		<20[c]	7.09	−0.39
HD 37507.....	49 Ori		211.2	−19.4	A4 V	40	−1SB0	170	4.80	0.13

[a] Distances shown are the distance of the Orion association subgroups when applicable (from Warren and Hesser 1978), or spectral distances calculated from stellar properties listed in the Bright Star Catalog (Hoffleit and Jaschek 1982). For the stars HD 35039, HD 35149, HD 37128, and HD 37492, the spectral distance and the subgroup distance are within 15% of each other. Values labeled with a colon are uncertain.

[b] Kindly classified for us by Nancy Houk from plates taken for the Michigan Spectral Catalogue (Houk 1978).

[c] Measured from these data.

[d] For spectral type B9 IV, the spectral distance of this star places it as a member of Ic.

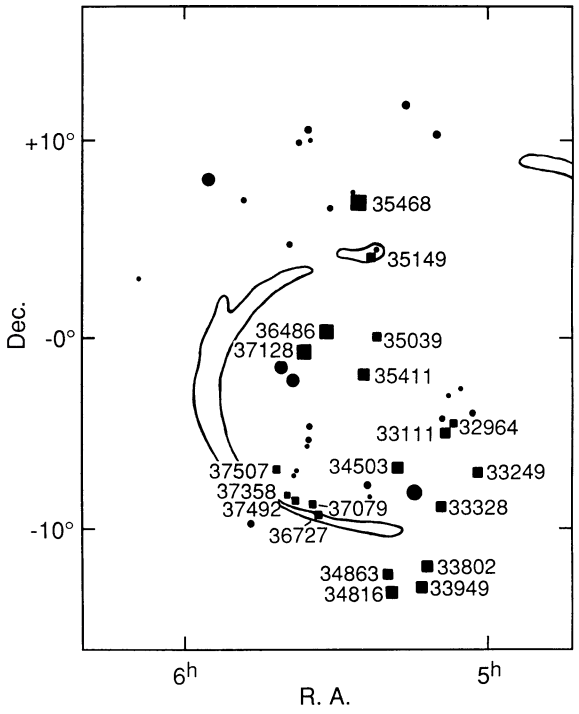

FIG. 1.—Diagram of the target stars plotted against a sketch of Barnard's Loop as seen in Hα emission and other stars in the Orion region. Target stars are identified by HD numbers. The size of the symbol increases with the star brightness. Square symbols indicate stars observed for this study, while circles are field stars with interstellar lines observed in other studies. The three nearby stars in front of the Orion superbubble, and which show OL 70 are HD 35468 (γ Ori), HD 34503 (τ Ori), and HD 33949 (κ Lep).

stars with observed interstellar lines are plotted as circles.) In order to sample interstellar matter on a relatively small spatial grid, stars of spectral class A and cooler must often be used as target stars, which may introduce uncertainties in correctly identifying interstellar versus weak sharp stellar absorption features. In principle this confusion can be avoided by selecting only rapidly rotating stellar targets, but in practice $v \sin i$ data are not available for the fainter stars observed for this program. We have estimated $v \sin i$ values for three program stars where these values were previously unavailable (Table 1).

The distance listed for a star is taken from the subgroup distances, if the star is a member of a subgroup of the Orion OB I association (Warren and Hesser 1978). Otherwise, distances are based on the spectral type of the star assuming a total to selective extinction ratio of $A_V/E(B-V) = 3$. Since the properties of interstellar grains in the Orion association region are anomalous (Johnson 1968), these spectral distances have some uncertainty. Where subgroup distances are listed, spectral distances are generally within 15% of the subgroup distance for the singe (nonbinary) stars. The velocities shown in column (3) of Table 2 and Figures 2, 3, and 4 are heliocentric (HC) velocities; velocities given in the local standard of rest coordinate system (LSR) are so indicated.

Optical observations of interstellar Na I and Ca II features were made using the echelle long camera on the 4 m telescope at Cerro Tololo Inter-American Observatory, during 1985 January and August. The CTIO data were acquired with a GEC CCD chip for the Na I D1 and D2 data and an RCA CCD chip for the Ca II H and K observations. These data have a signal-to-noise ratio greater than 250:1. All data were flat-fielded and reduced using the IRAF[3] software installed at the

[3] Developed by NOAO and publicly distributed.

TABLE 2

DATA FOR INTERSTELLAR LINES[a]

Star	Line[b]	v_{HC} (km s^{-1})	v_{LSR} (km s^{-1})	b (km s^{-1})	N[c] ($\times 10^{11}$ cm^{-2})	W_{tot} (mÅ)
HD 32249	Ca$^+$ (H)	12	−5	1	0.55	2.6:[d]
	Ca$^+$ (K)	14	−3	1	0.60:	3.2:[d]
HD 32964	Ca$^+$ (H)				<2	
	Ca$^+$ (K)			<0.21	<2	
HD 33111	Ca$^+$ (H)				<2	
	Ca$^+$ (K)			<0.21	<2	
HD 33328	Ca$^+$ (H)	5	−13	6	5.1	35 ± 3
	Ca$^+$ (H)	20	2	7	2.5	
	Ca$^+$ (K)	5	−13	6	5.2	70 ± 10
	Ca$^+$ (K)	20	2	8	3.1	
HD 33802	Ca$^+$ (H)				<2	
	Ca$^+$ (K)			<0.21	<2	
HD 33949	Ca$^+$ (H)				≤2	
	Ca$^+$ (K)	24	6	10	0.74	7 ± 2
HD 34503	Ca$^+$ (H)	26	8	6		2:
	Ca$^+$ (K)	26	8	6	0.4:	4:
	Na° (D$_1$)	29	11	3	2.5	23 ± 5
	Na° (D$_2$)	29	11	3	2.0	36 ± 5
HD 34816	Ca$^+$ (H)	2	−16	6	4.2	27 ± 4
	Ca$^+$ (H)	18	0	8	2.5	
	Ca$^+$ (K)	3	−15	6	4.6	64 ± 8
	Ca$^+$ (K)	20	2	10	3.0	
HD 34863	Ca$^+$ (H)				<2	
	Ca$^+$ (K)			<0.25	<2.5	
HD 35039	Ca$^+$ (H)	−1	−18	10		(53 ± 4)[e]
	Ca$^+$ (H)	15	−2	10		
	Ca$^+$ (K)	−1	−18	16		(150 ± 10)[e]
	Ca$^+$ (K)	15	−2	11		
HD 35149	Ca$^+$ (H)	9	−7	8	1.5	34 ± 3
	Ca$^+$ (H)	23	7	3	6.6	
	Ca$^+$ (K)	10	−6	8	1.2	56 ± 3
	Ca$^+$ (K)	23	7	3	6.6	
HD 35411	Ca$^+$ (H)	7	−10	7	2.4	17 ± 3
	Ca$^+$ (H)	23	6	10	1.2	
	Ca$^+$ (K)	8	−9	7	2.9	35 ± 8
	Ca$^+$ (K)	25	8	6	0.98	
HD 35468	Ca$^+$ (H)	21	5	9	1.7	8 ± 2
	Ca$^+$ (K)	21	5	9	1.6	15 ± 3
HD 36486	Ca$^+$ (H)	16	−1	12	3.1	21 ± 5
	Ca$^+$ (K)	15	−2	14	4.4	38 ± 5
HD 36727	Na° (D$_1$)	−9	−27	9	3.4	130 ± 11
	Na° (D$_1$)	5	−13	1	4.0	
	Na° (D$_1$)	21	3	1	16	
	Na° (D$_2$)	−8	−26	8	3.1	188 ± 13
	Na° (D$_2$)	6	−12	1	3.2	
	Na° (D$_2$)	20	2	2	13	
HD 37079	Na° (D$_1$)	1:	−17:	9:	1.0:	35 ± 4:[f]
	Na° (D$_1$)	20	2	4	4.3	
	Na° (D$_2$)	1	−17	9	1.2	80 ± 5:[f]
	Na° (D$_2$)	20	2	6	3.4	
HD 37128	Na° (D$_1$)	17	0	10	7.3	149 ± 9
	Na° (D$_1$)	30	13	9	9.0	
	Na° (D$_2$)	17	0	9	7.0	234 ± 10
	Na° (D$_2$)	30	13	8	6.6	
HD 37358	Na° (D$_1$)	5	−13	3	1.2	71 ± 6
	Na° (D$_1$)	20	2	2	8.1	
	Na° (D$_1$)	34	16	1	0.65	
	Na° (D$_2$)	5	−13	5	1.1	112 ± 8
	Na° (D$_2$)	20	2	2	7.5	
	Na° (D$_2$)	33	15	1	0.67	
HD 37492	Na° (D$_1$)	2	−16	1	1.1	84 ± 6
	Na° (D$_1$)	21	3	4	9.1	
	Na° (D$_2$)	4	−14	2	0.90	134 ± 9
	Na° (D$_2$)	21	3	5	8.0	
HD 37507	Na° (D$_1$)				<2	
	Na° (D$_2$)			<0.01	<2	

[a] Equivalent widths (col. [7]) and column densities (col. [6]) of stellar features are enclosed in parentheses. The variable v_{HC} gives the heliocentric velocity of the cloud component, while v_{LSR} gives the local standard of rest velocity. Values labeled with a colon are uncertain.

[b] Line data: Ca$^+$ (H) λ3968.468, $f = 0.341$; Ca$^+$ (K) λ3933.633, $f = 0.688$; Na° (D$_1$) λ5895.924, $f = 0.327$; Na° (D$_2$) λ5889.950, $f = 0.655$.

[c] A column density of N[Ca II(K)] = 2×10^{11} cm^{-2} corresponds to W[Ca II(K)] = 19 mÅ. A line with a column density of N[Na I(D2)] = 2×10^{11} cm^{-2} is partly saturated, so that the equivalent width of that line is a function of the Doppler value.

[d] Weak interstellar line superimposed on strong stellar line.

[e] Mainly or entirely stellar Ca II line in a low $v \sin i$ star.

[f] Strong initial telluric lines leading to possible systematic errors after telluric line removal.

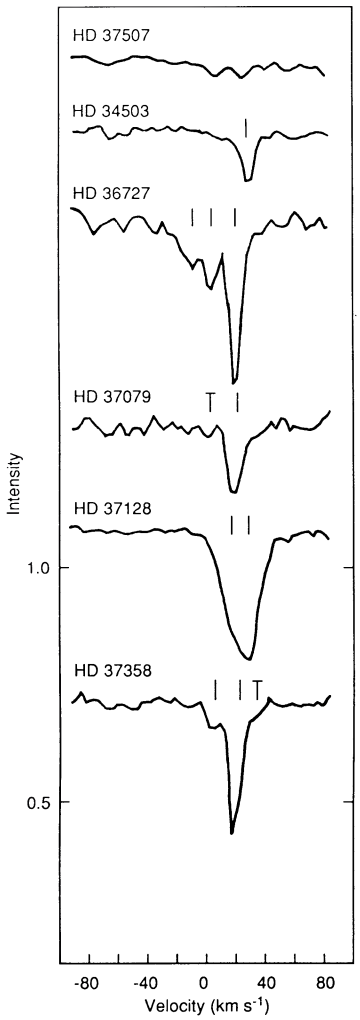

FIG. 2.—Interstellar Na I (D1) lines plotted in heliocentric velocity coordinates. Velocity components are marked with a vertical bar, and "T's" are features possibly contaminated by telluric absorption. The continua have been normalized to one. Numbers on the ordinate give the intensity with an arbitrary offset.

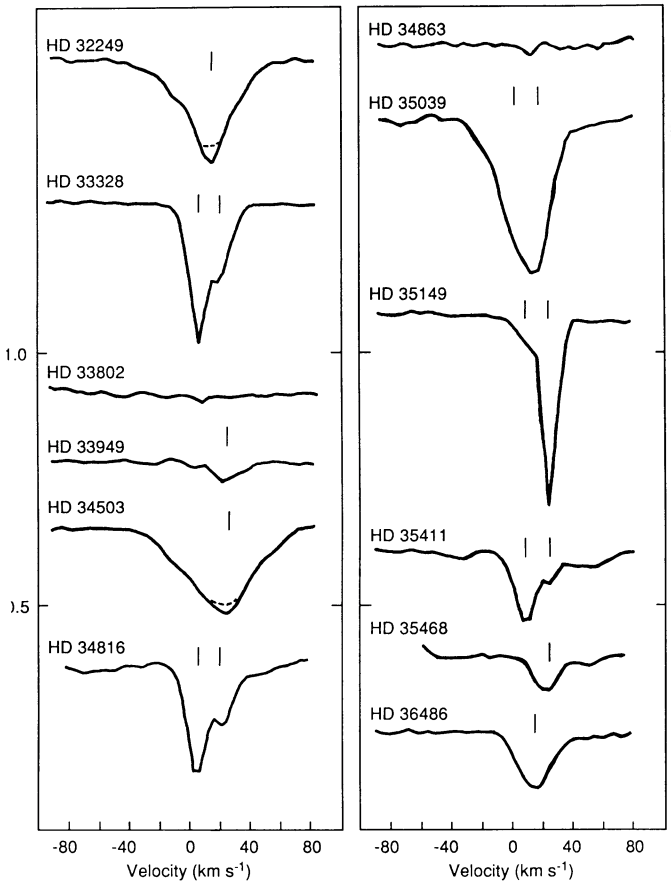

FIG. 3.—Interstellar Ca II (K) lines plotted in heliocentric coordinates. The continua have been normalized to one, except for HD 32249 and HD 34503 where the fitted stellar continua is shown with a dotted line. Numbers on the ordinate give the intensity with an arbitrary offset.

University of Chicago. Telluric features were removed from the sodium data by using the spectrum of the rapidly rotating star HD 37507 (49 Ori), which is located at 40 pc and has no detectable interstellar optical features, as a template for normalizing out telluric features. This normalizing technique works relatively well; any remaining telluric contamination in the profiles is noted with "T" in Figure 2.

Figures 2 and 3 show the interstellar Na I D1 and Ca II K absorption lines for these stars, after removal of stellar features. The stellar features were removed by fitting the continuum with a polynomial of order ≤ 5, and dividing by this polynomial. Once the interstellar absorption line profiles were determined, they were fitted with interstellar cloud components with internal velocity distributions described by a Maxwellian distribution. The fitted cloud components then gave the column density, Doppler width b, and velocity of each cloud component. The instrumental profile was assumed Gaussian with a FWHM of 8.4 km s^{-1}, a value derived from measurements of the comparison arc. Multiple interstellar clouds with velocity separation less than this value will blend and appear as a single cloud at the intermediate velocity measured here, but with a relatively large b value. Table 2 lists column densities, b values, velocities, and equivalent widths for the cloud components fit to these data. A 3 σ detection limit corresponds, roughly, to 1.3 mÅ (Ca II) or 2 mÅ (Na I). Typical errors in velocities in these data are ± 1 km s^{-1}. Our column densities for N(Ca II) in γ Ori and η Ori, and for N(Na I) in ϵ Ori, agree within the errors with previous values given by Hobbs (1974, 1978*b*).

In practice, unknown values of $v \sin i$, possible undetected binary companions, and possible circumstellar shell material combined with some uncertain spectral types, introduce uncertainties that must be considered when evaluating which spectral features are truly interstellar. The spectra of a few stars warrant individual mention. Ultimately, the identification of a feature as interstellar in a given target star must be confirmed by an observation of an interstellar feature at a similar velocity in a nearby star.

a) Stars at d < 150 pc

HD 32964, 66 Eri: This star is a binary, with relative orbital velocity of ~ 100 km s^{-1} (Hoffleit and Jaschek 1982). Both stars show stellar Ca II features, which in our data are separated by ~ 130 km s^{-1}.

HD 33949, κ Lep: This B9 V star at a spectroscopic distance of 70 pc shows a weak Ca II (K) absorption feature at $v_{HC} = 24$

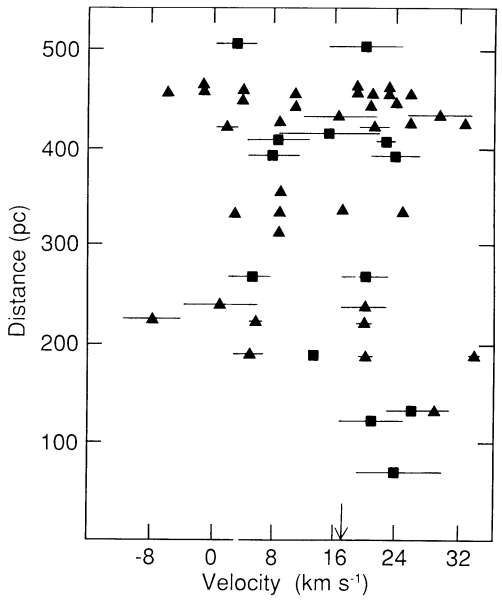

FIG. 4.—Heliocentric velocities of interstellar components seen in the target stars plotted against the stellar distances. Triangles represent interstellar Na I components while squares represent interstellar Ca II K components. Bars give the Doppler broadening constant, $\pm b/2$, for the component. Symbols plotted without any bars give interstellar components taken from Hobbs (1969, 1975, 1978*b*) and Marschall and Hobbs (1972). The arrow shows 0 km s^{-1} LSR.

km s^{-1} (Fig. 3). Since the stellar velocity listed in the *Bright Star Catalog* (Hoffleit and Jaschek 1982) is 18 km s^{-1}, and since the Ca II K velocity is at the velocity of OL 70 (Fig. 4), we tentatively identify this line as interstellar. However, this identification is qualified by the fact that κ Lep has been identified to have a "Vega-like" 60 μ infrared excess, and thus is a candidate for having a circumstellar disk or shell (Sadakane and Nishida 1986). Although Vega itself does not have a circumstellar Ca II (K) feature (to the 4 mÅ level), β Pic, a star with a well identified circumstellar disk, has a strong feature [W (Ca II K) = 97 mÅ] (Hobbs *et al.* 1985). Therefore, we cannot rule out the possibility that the κ Lep Ca II K feature is circumstellar. However, recent observations of Na I in κ Lep show two components, at $v_{HC} \sim 16$ and 23 km s^{-1} (Frisch and Fowler 1990). The $v_{HC} \sim 23$ km s^{-1} feature coincides in velocity with the Ca II feature, while the 16 km s^{-1} feature is near the stellar velocity. Based on these additional data, we conclude that the 24 km s^{-1} feature is interstellar, although the $v_{HC} \sim 16$ km s^{-1} seen in Na I may be either circumstellar or stellar.

HD 34503, τ Ori: Visual inspection of the Na I D profiles show a short wavelength asymmetry. The wings on the Na I main absorption feature are due to poorly corrected telluric lines (the exposure for this star was taken through clouds). There is a strong stellar Ca II component present in the profiles which makes continuum placement uncertain.

HD 35468, γ Ori: At our resolution, the weak interstellar Ca II feature is fit by a single cloud with a large Doppler constant, $b = 9$ km s^{-1}. At the higher spectral resolution of Hobbs (1978*a*), this feature shows a broad weak "flat-topped" profile at both the Na I D and Ca II K wavelengths, with absorption between 0 and 13 km s^{-1} (LSR).

b) Stars at d > 150 pc Stars

HD 32249, ψ Eri: The strong symmetric stellar features in the Ca II H, K profiles make it difficult to place the continuum correctly. The equivalent widths presented in the table are very uncertain but represent a lower limit if the marked interstellar feature exists.

HD 33328, λ Eri: The distance of this star is uncertain, since some reddening may occur in the atmosphere of this Be star (Houziaux and Manfroid 1987).

HD 34816, λ Lep: This star is outside of Barnard's Loop, and is the most distant star observed here. Weak absorption features are seen at high positive and negative velocities (-20 to -100 km s^{-1} and $+40$ to $+80$ km s^{-1}) in the Ca II K profile. The $+40$ to $+80$ km s^{-1} features appear not to have a Ca II H analogue, and may be stellar. The negative velocity features show up in both H and K, and we tentatively identify the weak -100 to -20 km s^{-1} absorption features as high-velocity Ca II. The possible UV counterpart of this gas may be absorption features in this velocity range seen in *Copernicus* Fe II λ1122.0 and Mg II λ1239.9 data (Bohlin *et al.* 1982), and in N I λ1199.5 and Si III λ1206.510 (Cowie *et al.* 1979). If the high positive velocity features are interstellar, then λ Lep may be sampling the back side of the superbubble.

HD 34863, ν Lep: The features in these profiles appear to be noise. However, if the 13 km s^{-1} dip in the Ca II K line profile is measured, an upper limit to the column density in the line of sight may be estimated at 2.5×10^{10} cm^{-2}, a factor of 3 below the strength of the feature seen in the star κ Lep, 2° away and at a distance of 70 pc. Tentatively, we conclude that OL 70 is patchy, with the interstellar Ca II column density changing by a factor of 3 over distance scales of $\lesssim 2$ pc. An alternative explanation would be that the spectral distance calculated at 187 pc for ν Lep (Table 1) is incorrect.

HD 35039, 22 Ori: The large, derived interstellar b values ($b > 10$ km s^{-1}) and low $v \sin i$ (14 km s^{-1}) for this spectroscopic binary star allow for the possibility that there may be stellar or circumstellar Ca II contributing to the profiles. The observed ratio of the total equivalent widths for the K and H lines is $W(\mathrm{K})/W(\mathrm{H}) = 2.8$, while a ratio of ≤ 2 is expected. This suggests that a stellar contribution to the features has interfered with the accurate modeling of the interstellar features. The short-wavelength asymmetry on the Ca II lines suggest either stellar mass loss or that the feature is the blend of stellar and interstellar components.

HD 35149, 23 Ori: These profiles show both broad and narrow interstellar components. The stellar $v \sin i$ rules out a stellar contribution to these lines. The b value (8 km s^{-1}) for the broad ($+10$ km s^{-1} HC) Ca II component may be from clouds unresolved in velocity space. This star is in the direction of maximum Hα emission from Barnard's Loop, which has an estimated temperature of 8000 $\pm$ 1000 K (RO). The star 23 Ori is distant enough (400 pc) to be behind at least some of the Hα emission. Of the two Ca II components, the strongest component at $v_{HC} = 23$ km s^{-1} ($+7$ km s^{-1} LSR) is at the velocity of the foreground gas, and the $v_{HC} = 10$ km s^{-1} (-10 km s^{-1} LSR) broad and weaker component is at the velocity of Barnard's Loop Hα emission of RO. At 8000 K, Ca would have a thermal broadening of 1.8 km s^{-1}, so most of the observed line width is from either the intrinsic velocity distribution of the gas clouds or from turbulence. The interstellar radical CH^+ is found in 23 Ori with $N(CH^+) = 8.8 \times 10^{12}$ cm^{-2} and $v_{LSR} = 6.5 \pm 0.2$ km s^{-1} (Federman 1982).

HD 35411, η Ori: A high-velocity feature at ~ 60 km s^{-1}

HC (~ 43 km s^{-1} LSR) is probably an unidentified stellar line, but weak absorption at -30 km s^{-1} HC (-47 km s^{-1} LSR) may be interstellar. Snow *et al.* (1979) report strong shell lines for this B1 + B2e binary. Oegerle and Polidan (1984) report this is a close binary pair with a period of ~ 8 days and a velocity semiamplitude of 145 km s^{-1}.

HD 36727: Three Na I components are present in this faint A9V star, which is in the direction of the Hα intensity maximum of Barnard's Loop. The negative velocity features suggest this star is behind the near side of the Orion superbubble, consistent with the general conclusions of this paper and the stellar distance.

HD 37128, ϵ Ori: The large b values for this star indicate unresolved velocity components; the absorption line data of Hobbs (1969), at a higher resolution, indicate clouds at $v_{HC} =$ 12, 18, and 25 km s^{-1}.

HD 37079, HD 37358, HD 37492: In the absence of $v \sin i$ or radial velocity data, possible stellar contributions to these profiles cannot be reliably eliminated. However, estimates of $v \sin i$ from our data are listed in Table 1 for HD 37358 and HD 37492. In HD 37492, the stellar features are narrow and may contribute weakly to the measured Na I features.

IV. ANALYSIS

In Figure 4, the Na I and Ca II velocity components listed in Table 2 are plotted against the stellar distance listed in Table 1, with calcium and sodium features plotted as squares and triangles, respectively. The bars on the velocity components show the Doppler velocities, $\pm b/2$, from Table 2. Points plotted without bars are measured from data from Hobbs (1969, 1974, 1975, 1976, 1978*b*) and Marschall and Hobbs (1972). These data show a bimodal velocity distribution. Target stars at distances ≤ 175 pc show foreground interstellar clouds centered at velocities of $v_{LSR} \sim 8 \pm 4$ km s^{-1} ($v_{HC} = 26 \pm 4$ km s^{-1}), while at greater distances interstellar clouds have velocities from $v_{LSR} \sim -25$ to $+17$ km s^{-1} ($v_{HC} = -7$ to 35 km s^{-1}). The distant negative velocity components are dominated by the energetics of the Orion superbubble, which is expanding towards the Sun (Menon 1958; Heiles 1976; RO), and are evidently formed in the shell material associated with the nearest side of the superbubble.

The nearby cloud at a velocity of $v_{LSR} \sim 8 \pm 4$ km s^{-1} ($v_{HC} \sim 26 \pm 4$ km s^{-1}) we identify as "OL 70", since observations of γ Ori, κ Lep and τ Ori show that the near side of this cloud must be located within 70 pc of the Sun. This distance is based on the assumptions that the feature identified in κ Lep is interstellar, and that the 70 pc spectroscopic distance listed in Table 1 for this star is correct. OL 70 must be patchy, however, since it is not seen in front of ν Lep, at 187 pc, and within 2° of κ Lep. This cloud is seen in both Na I D1 and D2, and Ca II H, K lines.

The distant positive velocity components evidently represent the superposition of absorption components from gas near the Orion stars embedded within the superbubble, and components of the foreground OL 70 cloud. Two arguments support the view that positive velocity gas is found within the Orion association. Studies of 21 cm emission in this region find that, at one position near the edge of the Ori-Eri superbubble, interstellar gas is accelerated from $v_{LSR} = +4$ km s^{-1} to -10 km s^{-1}. Baker (1973) found from a statistical analysis of H I 21 cm emission (which picked out features that vary strongly when compared with other H I emission within 3.5°) that interstellar gas at the position $l = 178°$, $b = -26°$ (feature "Tau HL-1"), had been accelerated from $v_{LSR} = +4$ km s^{-1} to -10 km s^{-1}. We interpret this to mean that $v_{LSR} = 4$ km s^{-1} represents the velocity of the undisturbed gas, which was then accelerated to -10 km s^{-1} by the expanding superbubble. Any dense clumps of gas embedded in the superbubble would remain at this velocity, as they would have been too massive to be accelerated by the superbubble shock fronts.

Additional evidence for positive velocity embedded gas shows up clearly in the Na I D absorption lines of ζ Ori AB and σ Ori AB in Figure 3 of Hobbs (1969). For each of these stars, a pair of *interstellar* Na I D absorption lines is found which mimics in appearance atmospheric Na I features seen in cool binary systems. The absorption features are seen at $v_{HC} = 23$, 26 km s^{-1} for ζ Ori AB ($v_{LSR} = 5$, 8 km s^{-1}) and at $v_{HC} = 21$, 24 km s^{-1} for σ Ori AB ($v_{LSR} = 3$, 6 km s^{-1}). These narrow absorption features cannot be from the atmospheres of the stars, which are B0 and O9.5 and have $v \sin i > 90$ km s^{-1}, and therefore must come from the surrounding nebulosity within the cluster. At distances of 450 pc, the AB members σ Ori and ζ Ori are separated by 0".2 and 2".4, respectively, corresponding to 0.0004 pc and 0.005 pc. The interstellar medium is inhomogeneous over such scales (e.g., Diamond *et al.* 1989), and it is easy to construct a scenario where the dense nebulosity close to the stars has independent density enhancements caused by the ram pressure of the stellar winds from each binary component, giving rise to a "binary" appearance in the Na I lines formed in the H II region. For instance, bow shocks such as seen around LL Ori and ζ Ori (Gull and Sofia 1979) may give rise to such features. Since for a constant radiation field the spatial density of Na I increases as the density squared (eq. [3]), denser regions in either H I or H II regions will yield increased Na I densities with respect to the surrounding regions.

The presence of positive velocity gas embedded in the Orion cluster means care must be taken when identifying OL 70 features in more distant stars.

a) OL 70

The properties of OL 70 can be deduced from the Na I data in nearby stars. In order to evaluate the ionization equilibrium in OL 70, we need an estimate of the radiation field specific to that cloud. Based on an estimated distance for OL 70 of 70 pc, OL 70 should be subject to a "standard" diffuse interstellar radiation field, since the nearest source of strong UV radiation, Orion OB I, is 300 pc distant. This assumption is supported by observations of the excited rotational levels of molecular hydrogen in δ Ori at $d = 400$ pc. This star shows an interstellar H_2 component at $v_{LSR} = 8.7$ km s^{-1} which has excitation that is typical for the UV field in the general neighborhood of the Sun (Spitzer and Morton 1976). Using H_2 equilibrium models of Jura (1974, 1975), Spitzer and Morton (1976) found that, for the $v_{LSR} \sim 8.7$ km s^{-1} cloud, the excited H_2 rotational level populations show a low ambient UV field, $\beta = 2 \times 10^{-10}$ s^{-1}, and a "best" value density, $n_{tot} \leq 3$ cm^{-3} (β is the rate for the radiative absorption by an H_2 molecule of a Lyman or Werner photon). In contrast, other velocity components in δ Ori and other Orion stars (including both positive and negative LSR velocities) show H_2 lines from different rotational levels that imply UV radiation fields factors of 5–80 higher, indicating that these clouds are closer to the background stars. The $v_{LSR} = 8.7$ km s^{-1} component in δ Ori may be behind OL 70, or correspond to OL 70 ($d_{OL\,70} \lesssim d_{8.7H_2}$). Since the more distant Orion stars dominate the radiation field in this direc-

tion, the OL 70 radiation field should be less than or equal to the field derived for that component.

Solving for the ionization equilibrium in OL 70, most sodium will be singly ionized so that

$$n(\mathrm{Na}^+) = \delta_{\mathrm{Na}} A_{\mathrm{Na}} n(\mathrm{H_{tot}}) , \quad (1)$$

and

$$\Gamma_{12} n(\mathrm{Na}^\circ) = \alpha_{21} \delta_{\mathrm{Na}} A_{\mathrm{Na}} n(\mathrm{H_{tot}}) n(e) . \quad (2)$$

The quantity $\Gamma_{12} = 2.1 \times 10^{-11}$ s^{-1} is the photoionization constant of Na I in the ambient Galactic radiation field. The quantity $\alpha_{21} = 5.73 \times 10^{-12}$ cm^3 s^{-1} is the radiative recombination rate between Na II and an electron at 100 K. We *assume* a temperature of 100 K for OL 70. The relatively large b values shown in Table 2, we believe, originate from unresolved velocity components. Since $\alpha \sim T^{-0.7}$, raising the temperature by a factor of 10 would reduce α by about a factor of 5. The quantities $n(\mathrm{Na}^\circ)$, $n(\mathrm{H_{tot}}) = n(\mathrm{H\ I}) + 2n(\mathrm{H_2})$, and $n(e) = \epsilon n(\mathrm{H_{tot}})$ cm^{-3} are the spatial densities of Na I, H I + 2H$_2$, and electrons, respectively. For ionization contributed mainly by the ionization of trace elements, $\epsilon = 5 \times 10^{-4}$. The quantity $A_{\mathrm{Na}} = 2.26 \times 10^{-6}$ is the cosmic abundance of sodium with respect to hydrogen, and δ_{Na} is the depletion factor of sodium (with possible values between 0 and 1). These values for the constants are taken from Frisch *et al.* (1987). The above relations give

$$n(\mathrm{Na}^\circ) = 3.1 \times 10^{-10} \delta_{\mathrm{Na}} n(\mathrm{H_{tot}})^2 . \quad (3)$$

Multiplying both sides by the cloud length, implicitly assuming that Na I and Na II are codistributed in space, gives

$$n(\mathrm{H_{tot}}) = 3.2 \times 10^9 \left[\frac{n(\mathrm{Na}^\circ)}{n(\mathrm{H_{tot}})}\right]\left[\frac{1}{\delta_{\mathrm{Na}}}\right] . \quad (4)$$

To our knowledge, the standard assumption that Na I and Na II are codistributed in space is untested by either observations or theory. Since the ionization potential of Na II is 47 eV, and the ionization potential of Na I is 5 eV, this question is worth further investigation.

We can use interstellar Na I column densities found for γ Ori and τ Ori to estimate the spatial density in OL 70. From Hobbs (1978*a*) and Savage and Jenkins (1972), we take values for N(Na I) and N(H I) for γ Ori and find $N(\mathrm{Na\ I})/N(\mathrm{H_{tot}}) = 1.11 \times 10^{-9}$, giving $n(\mathrm{H_{tot}}) \sim 3.6$ cm^{-3} for $\delta_{\mathrm{Na}} = 1$. This agrees with Hobbs (1978*a*) and is close to 3 cm^{-3}, the "best" upper limit set by the H_2 measurements toward δ Ori (Spitzer and Morton 1976) supporting the view that this cloud is cool. Raising the cloud temperature to 1000 K would increase the derived density to 18 cm^{-3}, in contradiction with the H_2 results. At a spatial density of 3 cm^{-3} and a column density of $\log N(\mathrm{H_{tot}}) = 19.81$ cm^{-2}, OL 70 would have a thickness of $\sim$7 pc. From the angular distribution of foreground stars showing absorption (20°), the width is at least 25 pc, indicating OL 70 is compressed in the sight line when compared to the angular extent on the sky. For dimensions $7 \times 15 \times 25$ pc^3 and density $n \sim 3$ cm^{-3}, OL 70 would have a mass of $\sim 200\ M_\odot$. We thus conclude that OL 70 is a relatively "standard" cool diffuse interstellar cloud, although the column density through the cloud is relatively low, $\log N(\mathrm{H\ I}) = 19.81$ cm^{-2}, in agreement with a similar conclusion reached by Hobbs (1978*a*). Hydrogen column densities are not available for τ Ori and κ Lep, the other two nearby stars which sample OL 70. For τ Ori, we estimate a column density of $\log N(\mathrm{H_{tot}}) = 20.37$ cm^{-2}, using the color excess $E(B-V) = 0.04$, and the standard ratio $N(\mathrm{H\ I} + 2\mathrm{H_2})/E(B-V) = 5.8 \times 10^{21}$ atoms cm^{-2} mag^{-1} (Bohlin *et al.* 1978). This gives $N(\mathrm{Na\ I})/N(\mathrm{H_{tot}}) = 8.62 \times 10^{-10}$ or $n_{\mathrm{tot}} = 2.81$ cm^{-3} for $\delta_{\mathrm{Na}} = 1$ and $T = 100$ K. This value for the spatial density, $n_{\mathrm{tot}} \sim 3$ cm^{-3}, is consistent with the value found above for γ Ori.

The picture regarding depletions in OL 70 is less clear. The Ca II/Na I ratio (Table 2 and Hobbs 1978*a*, 1978*b*) and Ti II data (Stokes 1978) indicate that depletion is relatively small in OL 70. The ratio of N(Ca II)/N(Na I) = 2.4 toward γ Ori indicates relatively high Ca II abundances, and the observed ratio $N(\mathrm{Ti\ II})/N(\mathrm{H\ I}) = 1.1 \times 10^{-9}$ in γ Ori gives a titanium abundance in this star a factor of 1.7 less depleted than the average Ti depletion for diffuse clouds. In contrast, N(Ca II)/N(Na I) ~ 0.2 in τ Ori indicates typical interstellar depletions, but the errors are larger here. Observations of Zn II, Fe II, Cr II, and Ni II using the *Hubble Space Telescope* would allow a direct measure of depletions and of the gas-to-dust ratio in this isolated interstellar cloud.

V. DISCUSSION

Beyond OL 70, the Orion superbubble, as defined by the Hα emission of Barnard's Loop (Sivan 1974) has dimensions 17° × 11°, or 135 × 85 pc^2 if centered at 450 pc. The extended Ori-Eri superbubble, as defined by RO from Hα and 21 cm emission data, however, has a diameter of $\sim$40°, or $\sim$300 pc if centered at 450 pc. If symmetric, the near side of the Ori-Eri superbubble would be at $\sim$300 pc. In our data, the multiplicity of velocity components at distances $\geq$200 pc, places the nearest side of this superbubble at $\sim$200 pc, indicating that it has expanded asymmetrically.

The prediction of Cowie *et al.* (1979) that "... the number of components of Na I or Ca II in a given star lying in this direction will not depend linearly on the distance of the star, but will increase rather abruptly at a distance from the Sun of 300–350 pc, and reach a plateau at greater distances" is fulfilled, except that we find the component number jump occurs at a smaller distance of 200 pc.

Cowie *et al.* (1979) found high-velocity ($v = -120$ km s^{-1}) low column density [$\log N(\mathrm{H}) < 10^{18}$ cm^{-2}] gas associated with the expanding Orion superbubble shell in front of 10 stars in this region. They concluded that this high-velocity gas was a radiative shock expanding into low-density gas, with the preshock gas having a density of $n_{\mathrm{tot}} \sim 0.003$ cm^{-3}. The expanding high-velocity shell apparently consists of material accelerated by both the Ori OB I and the λ Orion associations, with an age of $\sim$300,000 yr based on expansion velocity and size. The low density of 0.003 cm^{-3} for the preshock gas before this radiative shock cannot be the OL 70 cloud, which has a higher spatial density, $\sim$3 cm^{-3}. OL 70 must be a foreground object, separated by a gap from the nearest side of the expanding Ori-Eri superbubble.

Within the radiative shock is a lower velocity, denser shell of embedded higher density clouds ionized by the association stars. The visual absorption lines and 21 cm emission filaments seen at low velocities ($V \sim 20$ km s^{-1}) are identified with the expanding inner shell (Menon 1958; Heiles 1976; RO). Also, positive velocity gas that was too massive to be accelerated by the supernova events in Ori-Eri remains within the superbubble, in the region of association stars such as ζ Ori and σ Ori.

The pressure in OL 70, with $T \sim 100$ K, $n \sim 3$ cm^{-3} and zero magnetic field, is $P/k \sim 300$ K cm^{-3}. Snowden *et al.*

(1990) present an X-ray emission model which fills the local cavity with hot X-ray emitting gas at pressure $P/k \sim 9000$ K cm^{-3}. If the local cavity is in pressure equilibrium with OL 70, either a compensating magnetic field with strength $B \sim 5.5$ μG is present in OL 70, and magnetic pressure dominates thermal and turbulent pressure, or the local cavity is overpressurized with respect to OL 70. In the later case, the overpressurized plasma may dominate the kinematics of OL 70.

The location and motion of OL 70 can be used to evaluate two existing models of the kinematics of nearby interstellar gas. In the first model, an expanding H I shell associated with Gould's Belt is invoked to explain the kinematics of nearby H I (Lindblad *et al.* 1973; Olano 1982). OL 70 coincides in longitude, latitude and velocity with "Feature A", which is one segment of the expanding ring. However, neither Lindblad's original model (Lindblad *et al.* 1973) nor the recent Olano (1982) version place OL 70 at the correct distance. In the Lindblad *et al.* (1973) and Olano (1982) models, Feature A is located at a distance $\gtrsim 200$ pc, in disagreement with the $d \sim 70$ pc distance found here. In addition, these models do not explain the presence of nearby negative velocity gas (e.g., Frisch 1981) towards the region of Scorpius and Ophiuchus (in the opposite direction of the sky).

The alternative second model is to assume that OL 70 samples a linear flow of matter past the solar system, with the flow driven by the expanding Loop I supernova remnant (Frisch 1981; Crutcher 1982; Frisch and York 1986) centered in the opposite part of the sky ($l^\circ \sim 330^\circ$, $b \sim 20^\circ$). Positive velocity clouds at $d \sim 100$ pc towards Taurus, Lepus, and Orion place the tightest downwind constraints on this linear flow. The projected velocity using the local flow vector of Frisch and York (1986) toward OL 70 (γ Ori, τ Ori, and κ Lep) is $v_{\rm HC} = 26$ km s^{-1} ($v_{\rm LSR} = 8$ km s^{-1}). Each of these three stars show interstellar gas at this projected flow velocity. The relatively large b values found here (Table 2), however, suggest either a blending in velocity space of several clouds, or turbulence within the single OL 70 cloud.

If OL 70 is part of a local flow driven by the Loop I supernova event (or events), then the Loop I superbubble terminates at ~ 100 pc from the Sun in the Orion direction, having swept past the Sun and expanding to the greatest distance through the low density region surrounding the Sun. In this case, OL 70 may represent the gas swept up by the expanding shell. Also, the relative velocities between the Sun and OL 70 indicate that OL 70 would have swept past the Sun roughly 2 Myr ago. If the observed log N(H I) = 19.8 cm^{-2} of OL 70 were originally distributed over the 200 pc sight line between the center of the Loop I supernova remnant (130 pc away in Sco-Oph) and OL 70, it would have had an initial spatial density of 0.1 cm^{-3}. Since OL 70 includes gas at other velocities, and the expansion would not have been strictly linear, this is an upper limit for the initial density. If OL 70 contains interstellar gas swept up by an expanding supernova shell, we would expect to see reduced depletions in OL 70, but the data are not definitive here (§ IV).

Both the expanding ring model and the linear flow model have problems. In the first case, for instance, the OL 70 distance does not agree with the distance predicted by the Lindblad *et al.* (1973) model. In the second case, it is difficult to explain why interstellar matter should have a nearly linear flow vector over several hundred parsecs. The correct model may be a synthesis of these two models, whereby the Loop I supernova remnant expands in a preexisting cavity defined either by Gould's Belt, or, perhaps, the spiral wave density pattern. If OL 70 is the wall of this expanding shell, then turbulence in Na I and Ca II could simply be the wide range of motions expected in expanding OB I shells.

VI. CONCLUSIONS

Summarizing the results of this paper:

1. Stars closer than 190 pc towards the Orion association show only positive velocity interstellar features at $v_{\rm LSR} = 8 \pm 4$ km s^{-1}. These components arise in an interstellar cloud complex we designate OL 70, since they are seen in a star 70 pc distant, and in the Orion and Lepus constellations. The properties of OL 70 are consistent with $n_{\rm tot} \sim 3$ cm^{-3}, $T \sim 10^2$ K, and an average interstellar radiation field.

2. Beyond this distance (190 pc), both positive and negative velocity interstellar clouds are found, with the negative velocity components arising from the nearest side of the expanding Ori-Eri superbubble, and the positive velocity components from a superposition of gas in OL 70 and gas embedded in the superbubble. Based on H I 21 cm data and Hα emission data, the expansion of the inner Ori-Eri superbubble appears to have displaced positive velocity gas, a result consistent with our data. We find that the multiplicity of negative velocity components at distances ≥ 200 pc places the nearside of the superbubble at ~ 200 pc, indicating that it has expanded asymmetrically.

3. Since the radiative shock surrounding the Ori-Eri superbubble is expanding into low-density gas, $n \sim 0.003$ cm^{-3}, and densities in OL 70 are higher than this, there must be a gap between OL 70 and the expanding Ori-Eri superbubble complex. This gap is ≤ 100 pc, and the radiative shock is expanding at ~ 120 km s^{-1}. Therefore, in $\leq 1 \times 10^6$ yr, the expanding Ori-Eri superbubble will interact with OL 70.

4. Two possible models for the kinematics of OL 70 are that it is part of an expanding ring associated with Gould's Belt, or that it is part of a linear flow of material past the Sun driven by the Loop I supernova remnant. Both models have difficulties, and a synthesis of the two models may be more accurate. If OL 70 is correctly modeled as part of the local flow, then it must represent the boundary of the Loop I shell which has expanded asymmetrically. The swept-up gas by this shell would have had an initial spatial density of less than 0.1 cm^{-3}.

5. The pressure in OL 70 is a factor of 30 lower than the pressure in the X-ray plasma in the local cavity. A magnetic field with strength $B \sim 5.5$ μG in OL 70 would bring these two gases into pressure equilibrium. Otherwise, the overpressurized plasma may drive the motion of OL 70.

Several observations could further clarify the picture given here. High-resolution observations (0.5 km s^{-1}) of γ Ori, τ Ori, and κ Lep could explain the large b values found for OL 70 as small clouds within what may be an OL 70 complex or as turbulence over a large volume. The structure could be likewise clarified by finer sampling, using A, F, and G stars within the boundaries of Figure 1 and at distances of 100–200 pc. Observations of weak UV lines in the four stars mentioned earlier would allow depletions to be determined, which could shed light on the history of grains in OL 70. Measurements of the polarization of light from the stars required for finer sampling of OL 70 could also inform us as to the details of the magnetic field in this isolated cloud (or cloud complex). The isolated nature of this cloud makes it a candidate for testing the theory

that C IV and O VI come from evaporating cloud interfaces, since it is apparently surrounded by hot gas on all sides.

This research has been supported by NSF grant AST-83-17120 and NASA grants NAG5-704, NAG5-1303, and NAG5-286. We are happy to acknowledge the use of data sets compiled for the Local Interstellar Matter workshop project, and the support of Wayne Warren at the National Space Science Data Center in compiling some of these data sets. We also acknowledge using the SIMBAD data retrieval system (data base of the Strasbourg, France Astronomical Data Center) in the preparation of this research. An initial version of this work constituted the honors senior thesis of K. S. at the University of Chicago.

REFERENCES

Appenzeller, I. 1974, *Astr. Ap.*, **36**, 99.
Baker, P. L. 1973, *Astr. Ap.*, **26**, 204.
Barnard, E. E. 1895, *Pop. Astr.*, **2**, 151.
Bohlin, R. C., Hill, J. K., Jenkins, E. B., Savage, B. D., Snow, T. P., Spitzer, L., York, D. G. 1982, Wisconsin Astrophysics preprint No. 156.
———. 1983, *Ap. J. Suppl.*, **51**, 277.
Bohlin, R. C., Savage, B. D., and Drake, J. F. 1978, *Ap. J.*, **224**, 132.
Cowie, L. L., Songaila, A., and York, D. G. 1979, *Ap. J.*, **230**, 459.
Crutcher, R. M. 1982, *Ap. J.*, **254**, 82.
Diamond, P. J., Goss, W. M., Romney, J. D., Booth, R. S., Kalberla, P. M. W., and Mebold, U. 1989, *Ap. J.*, **347**, 302.
Federman, S. R. 1982, *Ap. J.*, **257**, 125.
Frisch, P. C. 1981, *Nature*, **193**, 377.
Frisch, P. C., and Fowler, J. R. 1990, in preparation.
Frisch, P. C., and York, D. G. 1983, *Ap. J. (Letters)*, **271**, L59.
———. 1986, *The Galaxy and the Solar System* (Tucson: University of Arizona Press).
Frisch, P. C., York, D. G., and Fowler, J. R. 1987, *Ap. J.*, **320**, 842.
Gull, T. R., and Sofia, S. 1979, *Ap. J.*, **230**, 782.
Heiles, C. 1976, *Ap. J. (Letters)*, **208**, L137.
———. 1984, *Ap. J. Suppl.*, **55**, 585.
Hobbs, L. M. 1969, *Ap. J.*, **157**, 135.
———. 1974, *Ap. J.*, **191**, 381.
———. 1975, *Ap. J.*, **202**, 628.
———. 1976, *Ap. J.*, **206**, L117.
———. 1978*a*, *Ap. J.*, **222**, 491.
———. 1978*b*, *Ap. J. Suppl.*, **38**, 129.
Hobbs, L. M., Vidal-Madjar, A., Ferlet, R., Albert, C. E., and Gry, C. 1985, *Ap. J. (Letters)*, **293**, L29.
Hoffleit, D., and Jaschek, C. 1982, *The Bright Star Catalogue* (New Haven: Yale Univ. Obs.).
Houk, N. 1978, *Michigan Catalogue of Two-Dimensional Spectral Types of HD Stars* (Ann Arbor: University of Michigan, Department of Astronomy).
Houziaux, L., and Manfroid, J. 1987, *Physics of Be Stars*, ed. A. Slettebak and T. P. Snow (Cambridge: Cambridge Univ. Press), p. 172.
Hu, E. 1981, *Ap. J.*, **248**, 119.
Isobe, S. 1973, in *IAU Symposium 52: Interstellar Dust and Related Topics*, ed. J. M. Greenberg and H. C. Van de Hulst (Dordrecht: Reidel), p. 230.
Jenkins, E. B. 1978, *Ap. J.*, **219**, 856.
———. 1987, *Interstellar Processes*, ed. D. J. Hollenbach and H. A. Thronson (Dordrecht: Reidel), p. 533.
Johnson, H. L. 1968, *Nebulae and Interstellar Matter*, ed. B. M. Middlehurst and L. H. Allen (Chicago: University of Chicago Press), p. 167.
Jura, M. 1974, *Ap. J.*, **191**, 375.
———. 1975, *Ap. J.*, **197**, 575.
Lindblad, P. O., Grape, K., Sandquist, A., and Sehober, J. 1973, *Astr. Ap.*, **24**, 309.
Lucke, P. B. 1978, *Astr. Ap.*, **64**, 367.
Maddalena, R. J., Morris, M., Moscowitz, J., and Thaddeus, P. 1986, *Ap. J.*, **303**, 375.
Marschall, L. A., and Hobbs, L. M. 1972, *Ap. J.*, **173**, 43.
Menon, T. K. 1958, *Ap. J.*, **127**, 28.
Nousek, J. A., Fried, P. M., Sanders, W. T., and Kraushaar, W. L. 1982, *Ap. J.*, **258**, 83.
O'Dell, C. R., York, D. G., and Heinze, K. G. 1967, *Ap. J.*, **150**, 835.
Oegerle, W. R., and Polidan, R. S. 1984, *Ap. J.*, **285**, 648.
Olano, C. A., 1982, *Astr. Ap.*, **112**, 195.
Paresce, F., Jakobsen, P., and Bowyer, S. 1983, *Astr. Ap.*, **124**, 300.
Perry, C. L., Johnson, L., and Crawford, P. L. 1983, *Astr. J.*, **87**, 1751.
Pettini, M., Boksenberg, A., Bates, B., McCaughan, R. F., and McKeith, C. D. 1977, *Astr. Ap.*, **61**, 839.
Pickering, W. H. 1890, *Sidereal Messenger*, **9**, 2.
Reich, W. 1978, *Astr. Ap.*, **64**, 407.
Reynolds, R. J. 1988, *Ap. J.*, **333**, 341.
Reynolds, R. J., and Ogden, P. M. 1979, *Ap. J.*, **229**, 942 (RO).
Sadakane, K., and Nishida, M. 1986, *Pub. A.S.P.*, **98**, 685.
Savage, B. D., Bohlin, R. C., Drake, J. F., and Budich, W. 1977, *Ap. J.*, **216**, 291.
Savage, B. D., and Jenkins, E. B. 1972, *Ap. J.*, **172**, 491.
Sivan, J. P. 1974, *Astr. Ap. Suppl.*, **16**, 163.
Sivan, J. P., Stasinska, G., and Lequeux, J. 1986, *Astr. Ap.*, **158**, 279.
Snow, T. P., Peters, G. J., and Mathier, R. D. 1979, *Ap. J. Suppl.*, **39**, 359.
Snowden, S. L., Cox, D. P., McCammon, D., and Sanders, W. T. 1990, *Ap. J.*, **354**, 200.
Spitzer, L., Drake, J. F., Jenkins, E. B., Morton, D. C., Rogerson, J. B., and York, D. G. 1973, *Ap. J. (Letters)*, **181**, L116.
Spitzer, L., and Morton, W. A. 1976, *Ap. J.*, **204**, 731.
Stokes, G. M. 1978, *Ap. J. Suppl.*, **36**, 115.
Troland, T. H., and Heiles, C. 1982, *Ap. J. (Letters)*, **260**, L19.
Warren, W. H., and Hesser, J. E. 1978, *Ap. J. Suppl.*, **36**, 497.

P. C. FRISCH and D. G. YORK: University of Chicago, Department of Astronomy and Astrophysics, 5640 S. Ellis, Chicago, IL 60637

K. SEMBACH: University of Wisconsin, Washburn Observatory, Department of Astronomy, 475 N. Charter St., Madison, WI 53706